ICSV14
Cairns • Australia
9-12 July, 2007
14th International Congress on Sound & Vibration

RESEARCH ON THE THEORIES OF BEM BASED CYCLOSTATIONARY NEAR FIELD ACOUSTIC HOLOGRAPHY

Haibin Zhang, Weikang Jiang and Quan Wan

State Key Laboratory of Mechanical System and Vibration, Shanghai Jiaotong University
No.800, Dongchuan Road, Shanghai 200240, P. R. China, wkjiang@sjtu.edu.cn

Abstract

The cyclo-stationary vibrational signal modulated by other signals is an example of a non-stationary signal found frequently in internal combustion engines and rotating machinery. The modulation frequency component may be extracted from the total signal using second order cyclic statistics. In previous research, the authors used the cyclo-stationary near field acoustic holography (CYNAH) technique in which the cyclic spectral density functions were used to reconstruct physical quantities. In this paper the CYNAH method is combined with the boundary element method to overcome the limitations of the planar CYNAH method. The methods used in the conventional BEM based NAH to overcome non-uniqueness and the ill-posed nature of the reconstruction are also implemented here. Results of a simulation show satisfactory agreement between computed and analytical values.

1. INTRODUCTION

The nearfield acoustic holography (NAH) [1] was developed quickly to reconstruct the sound field in last twenty years. The NAH algorithms were developed in some different ways by combining with the different algorithms. Fast Fourier's transfer (FFT) approach is implemented for radiating sources with simple profiles [1-2] which requires the source boundary to match the separable geometries of the acoustic wave equation such as planar, cylindrical and spherical geometries. The boundary element method (BEM) and singular value decomposition (SVD) were applied to reconstruct the sound field radiated from the sources with irregular profiles [3-4]. The Helmholtz's equations least squares (HELS) [5] and wave superposition algorithms (WSA) [6] could be considered as the equivalent source method, which were also illustrated useful for 3-dimensional complicated sources. All these NAH methods reconstructed the sound field in the frequency or wave-number domain. Some researchers reconstructed the sound field in a range of the continuous frequency on the source surface and then obtained the transient sound information in time domain via inverse FFT [7]. This method was utilized to locate the brake squeal noise sources and engine knocking noise.

The cyclo-stationary signal modulated seriously by other signal is a special example of the non-stationary signal, which is found frequently in the rotating machinery. The modulating wave components are usually resulted from periodic pulse vibration, while the carrier wave components are resulted from the free oscillation or other random disturbance. The cyclic statistics of the cyclostationary signals [8-9] such as cyclic spectral density (CSD) are applied for diagnosing some machinery faults. The types and mechanism of mechanical fault can be diagnosed by analyzing the single channel of cyclo-stationary signal. Reconstructing the cyclostationary sound field on the machine surface will supply much information for diagnosing the faults such as location and type of mechanical faults.

An algorithm named cyclo-stationary nearfield acoustic holography (CYNAH) [10-11] was suggested to reconstruct the cyclostationary sound field on a planar source surface. The CSD hologram by CYNAH shows the feature and location of modulating wave, since the CSD function is able to decompose the modulating wave and carrier wave. In order to reconstruct the cyclostationary sound field for irregularly shaped sources, the CYNAH based on BEM is presented here.

2. THE DERIVATION OF BEM-BASED CYNAH THEORY

2.1 NAH based on BEM in the stationary sound field

Helmholtz's integral equation is the foundation of the NAH algorithm based on BEM for stationary sound field, which can be evaluated as follows:

$$C \cdot p(r) = \int_{S_s} \left(p(r_s) \frac{\partial}{\partial n_s} G(r, r_s) - i\rho\omega\, v_n(r_s) G(r, r_s) \right) dS_s \tag{1}$$

with

$$C = \begin{cases} 1 & r \in V_f \ , \\ 0 & r \in V_s \ , \\ 1/2 & r \in S_s \ , \quad \mathrm{S_s} \text{ is a smooth surface} \\ \Omega / 4\pi & r \in S_s \ , \quad \mathrm{S_s} \text{ is a nonsmooth surface} \end{cases}$$

where, $p(r)$ means the complex pressure in the field, $p(\mathrm{r_s})$ and $v_n(\mathrm{r_s})$ mean the pressure and the normal velocity on the surface, respectively. V_s and V_f imply the interior volume and the exterior volume, respectively. S_s denotes the boundary. $G(r, r_s) = e^{jk|r-r_s|} / 4\pi \,|\, r - r_s \,|$ is the free-space Green's function with wave number $k=\omega/c$, where ω and c represent the angular frequency and wave speed, respectively. n_s denotes the outward normal direction to the source surface. The coefficient C depends on the boundary smoothness. Ω denotes the solid angle.

Equation (1) can be solved numerically by discretizing the boundary S_s into elements and employing the shape function. Two matrix equations are formed including surface solution and field solution as follows:

$$CP_s = D_{ss} P_s - M_{ss} V_{ns} \tag{2}$$

$$P_h = D_{hs} P_s - M_{hs} V_{ns} \tag{3}$$

where, P_h and P_s are the vectors corresponding to the measured sound pressure on the hologram and the unknown pressure on the surface, respectively. V_{ns} means the normal velocity on the surface. The subscript h and s denote the hologram and the source surface, respectively. D_{ss}, M_{ss}, D_{hs} and M_{hs} are the transfer matrixes.

The relations between the hologram pressure and the surface pressure or the normal velocity can be built as follows:

$$P_h = [D_{hs} \overline{D}_{ss}^{-1} M_{ss} - M_{hs}] V_{ns} \tag{4}$$

$$P_h = [D_{hs} - M_{hs} M_{ss}^{-1} \overline{D}_{ss}] P_s \tag{5}$$

where, $\overline{D}_{ss} = (D_{ss} - C \cdot I)$ with I meaning the identity matrix. Then, the pressure and the normal velocity on the surface can be obtained in an inversely process.

2.2 Cyclo-stationary : definition and properties

The definitions of cyclo-stationary can be found in many papers and books about signal processing. Usually, a random signal $u(t)$ is considered as n^{th} order cyclo-stationary if its time-domain n^{th} order moment is a periodical function of the time, t [8].

The second-order cyclo-stationarity, which is recently applied in mechanical fault diagnosis, is discussed as follows. The second-order cyclic statistical quantities, cross-CSD functions, are used as the transform variable in CYNAH method. The CSD function can be evaluated in temporal or frequency viewpoint. The basic equation of second-order cross-CSD in the frequency domain is introduced as follows:

$$S_{uv}^{\alpha}(f) = \left\langle U(f+\alpha/2) \cdot V^{*}(f-\alpha/2) \right\rangle_t \tag{6}$$

where the operator $\langle \cdot \rangle_t$ and superscript $*$ denote the time-average and the conjugate operator, respectively. $U(f+\alpha/2)$ and $V(f-\alpha/2)$ represent the spectral components of cyclo−stationary signal $u(t)$ and $v(t)$ at frequencies $f+\alpha/2$ and $f-\alpha/2$, respectively. The frequency α is the cyclic frequency.

According to the filter property of CSD, CSD can be obtained by a pair of cross-CSD as follows:

$$S_{uu}^{\alpha}(f) = S_{uv}^{\alpha}(f) S_{vu}^{\alpha}(f) \big/ S_{vv}^{\alpha}(f) \tag{7}$$

2.3 CYNAH based on BEM for cyclo-stationary sound field

If the radiating sound signal is cyclo-stationary, the spectrum of modulating wave and carrier wave are mixed up in the PSD figure, and they can not be decomposed in the reconstructed sound field by current NAH method. The cyclic statistic of cyclo-stationary signal is changing periodically and containing the information of the modulating wave, which is helpful to diagnose some mechanical fault.

Reconstructing the CSD function on the surface from the CSD function on the hologram can not be implemented directly because of the lack of phase information of CSD function. However, the cross-CSD function contains the phase information between surface and hologram. Therefore, using equation (7) to obtain CSD after reconstructing the cross-CSD function on the surface firstly will be a good choice. Supposing a channel of pressure signal on some field point as the reference, its spectrum $p(r_{\mathrm{ref}}, f, t)$ depends on time because of the non-stationary nature. The equation (1) can be written as follows by multiplying $p(r_{ref}, f, t)$ to both sides:

$$\begin{aligned} & C \cdot p(r, f+\alpha/2, t) p^{*}(r_{ref}, f-\alpha/2, t) \\ & = \int_{S_s} p(r_s, f+\alpha/2, t) p^{*}(r_{ref}, f-\alpha/2, t) \cdot \frac{\partial}{\partial n_s} G(r, r_s, f+\alpha/2) \\ & \quad - v_n(r_s, f+\alpha/2, t) p^{*}(r_{ref}, f-\alpha/2, t) \cdot [j2\pi\rho(f+\alpha/2) G(r, r_s, f+\alpha/2)] dS_s \end{aligned} \tag{8}$$

where the superscript $*$ denotes the conjugate operator, and α means the cyclic frequency. Although the hidden parameter of frequency f in free-space Green's function is exhibited in equation (8), the actual meaning and expression of Green's function is the same as that in equation (1). Temporal factor comes up in the expression of the spectral component of the pressure and the normal velocity. It stresses the non-stationary feature of cyclo-stationary signal and indicates the temporal variation of spectral components. According to the cyclo-stationary theory, equation (8) will be expressed by cross-CSD functions by time-averaging the both sides with time *t* as following:

$$\begin{aligned} CS_{pr}^{\alpha}(r,f) = \int_{S_s} & S_{sr}^{\alpha}(r_s,f)\cdot\frac{\partial}{\partial n_s}G(r,r_s,f+\alpha/2) \\ & -V_{sr}^{\alpha}(r_s,f)\cdot j2\pi\rho(f+\alpha/2)G(r,r_s,f+\alpha/2)dS_s \end{aligned} \tag{9}$$

where S_{pr}^{α}, S_{sr}^{α} and V_{sr}^{α} denote the cross-CSD functions at the frequency *f* with the cyclic frequency α, respectively. In the same way, the other derivation among comparative series of cross-CSD functions can be described as follows:

$$\begin{aligned} & C\cdot p^{*}(r_{ref},f+\alpha/2,t)p(r,f-\alpha/2,t) \\ & = \int_{S_s} p^{*}(r_{ref},f+\alpha/2,t)p(r_s,f-\alpha/2,t)\cdot[\frac{\partial}{\partial n_s}G(r,r_s,f-\alpha/2)] \\ & \quad - p^{*}(r_{ref},f+\alpha/2,t)v_n(r_s,f-\alpha/2,t)\cdot[j2\pi\rho(f-\alpha/2)G(r,r_s,f-\alpha/2)]dS_s \end{aligned} \tag{10}$$

Time-averaging the both sides of equation (10), equation (11) can be obtained below:

$$\begin{aligned} CS_{rp}^{\alpha^*}(r,f) = \int_{S_s} & S_{rs}^{\alpha^*}(r_s,f)\cdot[\frac{\partial}{\partial n_s}G(r,r_s,f-\alpha/2)] \\ & -V_{rs}^{\alpha^*}(r_s,f)\cdot[j2\pi\rho(f-\alpha/2)G(r,r_s,f-\alpha/2)]dS_s \end{aligned} \tag{11}$$

Comparing the equation (9) and (1), it can be found that the two equations are similar to each other except that the second-order statistical quantities take the place of the pressure and the normal velocity. Thus, all procedures applied to BEM-based NAH, including discretizing the boundary surface, utilizing the isoparametric quadratic shape function and assembling series of linear equations into matrix mode, can also be implemented to equation (9). These procedures will not be introduced in detail here. The relationship between a series of cross-CSD function vectors, involved equation (9), will be given directly. The relationship among the cross-CSD functions, surface-to-hologram and surface-to-surface, can be determined by two equations as follows:

$$\left[S_{pr}^{\alpha}\right] = \left[D_{hs}(f+\alpha/2)\right]\left[S_{sr}^{\alpha}\right] - \left[M_{hs}(f+\alpha/2)\right]\left[V_{sr}^{\alpha}\right] \tag{12}$$

$$C\left[S_{sr}^{\alpha}\right] = \left[D_{ss}(f+\alpha/2)\right]\left[S_{sr}^{\alpha}\right] - \left[M_{ss}(f+\alpha/2)\right]\left[V_{sr}^{\alpha}\right] \tag{13}$$

where, $[S_{pr}^{\alpha}]$, $[S_{sr}^{\alpha}]$ and $[V_{sr}^{\alpha}]$ are the cross-CSD function vectors at the frequency *f* with the cyclic frequency α between field pressure, surface pressure and surface normal velocity to the reference signal, respectively. $[D_{hs}(f+\alpha/2)]$ and $[M_{hs}(f+\alpha/2)]$ are dipole and monopole transfer matrixes between the hologram and the source surface, respectively. $[D_{ss}(f+\alpha/2)]$ and $[M_{ss}(f+\alpha/2)]$ are the dipole and the monopole transfer matrices from source surface to itself analogously. It can be found that the transfer matrices are similar between the CYNAH and NAH except for the frequency shift.

The succinct expressions with concealed frequency (*f*+α/2) for transfer matrixes are obtained as follows:

$$\left[S_{pr}^{\alpha}\right] = \left[D_{hs} - M_{hs}M_{ss}^{-1}\overline{D}_{ss}\right]\cdot\left[S_{sr}^{\alpha}\right] = \left[G_p\right]\cdot\left[S_{sr}^{\alpha}\right] \tag{14}$$

$$\left[S_{pr}^{\alpha}\right] = \left[D_{hs}\overline{D}_{ss}^{-1}M_{ss} - M_{hs}\right]\cdot\left[V_{sr}^{\alpha}\right] = \left[G_v\right]\cdot\left[V_{sr}^{\alpha}\right] \tag{15}$$

where $\overline{D}_{ss} = (D_{ss} - CI)$ with *I* being an identity matrix. This pair of resultant system equations builds the relationship between $[S_{pr}^{\alpha}]$ and $[S_{sr}^{\alpha}]$ or $[V_{sr}^{\alpha}]$. $[S_{sr}^{\alpha}]$ and $[V_{sr}^{\alpha}]$ can be obtained inversely via equations (16) and (17) as follows:

$$\left[S_{sr}^{\alpha}\right]=\left[G_{p}\right]^{-1}\left[S_{pr}^{\alpha}\right] \tag{16}$$

$$\left[V_{sr}^{\alpha}\right]=\left[G_{v}\right]^{-1}\left[S_{pr}^{\alpha}\right] \tag{17}$$

Another pair of matrix equations can be derived in the similar way, and its succinct expression with concealed frequency (f−α/2) for transfer matrixes are as follows:

$$\left[S_{rs}^{\alpha}\right]^{*}=\left[G_{p}\right]^{-1}\left[S_{rp}^{\alpha}\right]^{*} \tag{18}$$

$$\left[V_{rs}^{\alpha}\right]^{*}=\left[G_{v}\right]^{-1}\left[S_{rp}^{\alpha}\right]^{*} \tag{19}$$

where, $\left[S_{rp}^{\alpha}\right]$, $\left[S_{rs}^{\alpha}\right]$ and $\left[V_{rs}^{\alpha}\right]$ are the comparative cross-CSD function vectors at frequency f with cyclic frequency α relative to $[S_{pr}^{\alpha}]$, $[S_{sr}^{\alpha}]$ and $[V_{sr}^{\alpha}]$, respectively. The corresponding frequencies in different transfer matrixes and conjugate operator are fallible if carelessness.

The CSD vector of the pressure on the surface can be obtained after the harvest of a pair of cross-CSD vectors of between the pressure on the surface and the reference. So the CSD vector of the pressure on the surface does. The CSD function on the i^{th} surface node, at the frequency f with the cyclic frequency α, can be evaluated by equation (20) and (21) as follows:

$$S_{ssi}^{\alpha}=S_{sri}^{\alpha}\cdot S_{rsi}^{\alpha}\big/S_{rr}^{\alpha} \tag{20}$$

$$V_{ssi}^{\alpha}=V_{sri}^{\alpha}\cdot V_{rsi}^{\alpha}\big/S_{rr}^{\alpha} \tag{21}$$

where, S_{rr}^{α} is the CSD function of the reference signal, subscript i means the i^{th} element of vectors corresponding to the i^{th} node. Thus, the surface CSD functions of either pressure or normal velocity are obtained and CSD at any point on the surface can be evaluated via the shape function.

By comparing the BEM-based CYNAH and the BEM-based NAH, it can be found that the ill-posed nature and non-uniqueness problems also occur in the CYNAH algorithm. Therefore, the truncated SVD (singular value decomposition) procedure [12] is adopted to overcome the ill-posed nature in CYNAH. The combined Helmholtz's integral equation formulation (CHIEF) method [13] is implemented to eliminate the non-uniqueness problem happening on the problematic frequency.

3. SIMULATION STUDY OF CYNAH ALGORITHM BASED ON BEM

3.1 Simulation

A numeric simulation case is studied in this section to verify CYNAH algorithm based on BEM. It is a cylinder with two spherical end-caps enclosing a finite length line source inside, which determines the normal velocity and pressure on the cylinder surface (see figure1). The pulsating signals of the line sources are cyclostationary. The reason of choosing this numeric case is that the facility of synthetically generating pressure and normal velocity for locations collocated on surface and hologram. Figure 2 is the diagram of the portion of the cylinder with two spherical end-caps, including 40 elements and 122 nodes. The input parameters are selected as r_0=0.3m, a=0.01m, and length L=0.5m.

The vibrating velocity signal on the finite-length line source in temporal mode is evaluated by equation (22) as follows:

$$v(t)=a(t)\cdot\cos(2\pi f_a t) \tag{22}$$

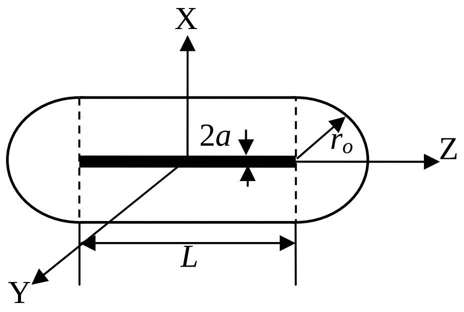

Figure 1. Cylinder radiator with spherical end-caps spherical enclosing linear cyclostationary vibrator.

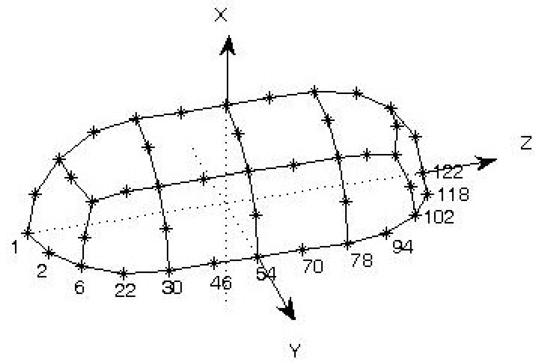

Figure2. The partition plot of cylinder with two end-caps, 40 elements and 122 nodes

where $a(t)$ is a purely stationary random signal with zero mean and f_a=200 Hz. The velocity signal is a cyclostationary amplitude-modulation (AM) signal with the unique cyclic frequency 400 Hz. The carrier wave $\cos(2\pi f_a t)$ is modulated by $a(t)$. It is easy to see that the spectrum of modulation signal a(t) becomes two sidebands around f_a under the effect of carrier wave by means of comparing the PSD drawings of $v(t)$ and $a(t)$ as shown in figure 3(a) and (b). In figure 3(c), the CSD function of $v(t)$ removes the disturbance of carrier wave and extracts the characteristics of modulation wave $a(t)$ solely.

The normal velocity and the pressure on the surface and hologram can be evaluated by equations (23) and (24) as follows:

$$p(r,k) = j\frac{\rho_0 cU(k)ka}{2}\int_{-L/2}^{L/2}\frac{1}{|r-z|}e^{jk|r-z|}dz \tag{23}$$

$$v_n(r,k) = \frac{U(k)a}{2}\int_{-L/2}^{L/2}\frac{jk|r-z|-1}{|r-z|^2}e^{jk|r-z|}\frac{\partial|r-z|}{\partial n}dz \tag{24}$$

where, r means the coordinate of surface point or field point, z means the coordinate of point on line source, a means the radius of the line source with the finite length L, n is the outward normal direction. $U(k)$ in the equation (23) and (24) is the normal velocity on the line source surface. The PSD of the sound pressure radiated from the source is shown in figure 4(a), which is a little different from the PSD of $v(t)$ in figure 3(b) because of the influence of transfer function. However, the sound pressure is still cyclostationary. The CSD of the sound pressure at α=400 Hz is shown in figure 4(b), and the spectral characteristics of the modulating components are shown clearly.

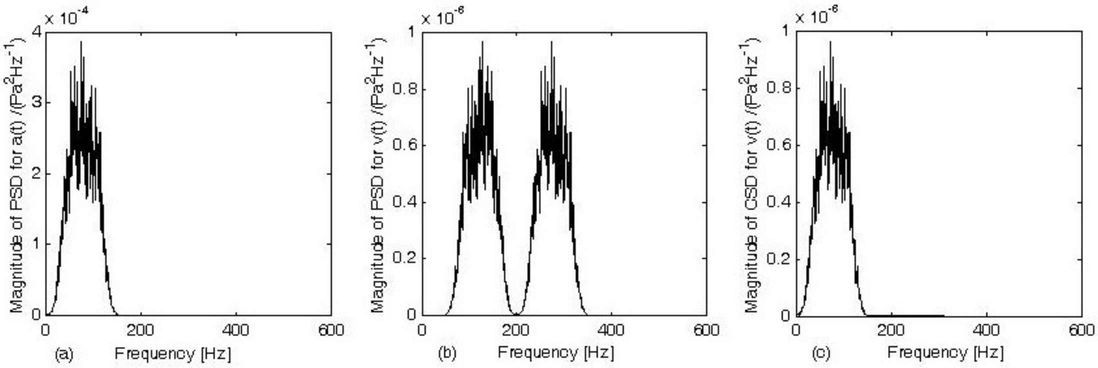

(a). The PSD plot of $a(t)$ (b) The PSD plot of $v(t)$ (c) The CSD plot of $v(t)$, α=400 Hz

Figure 3. Analysis of the simulation velocity signal

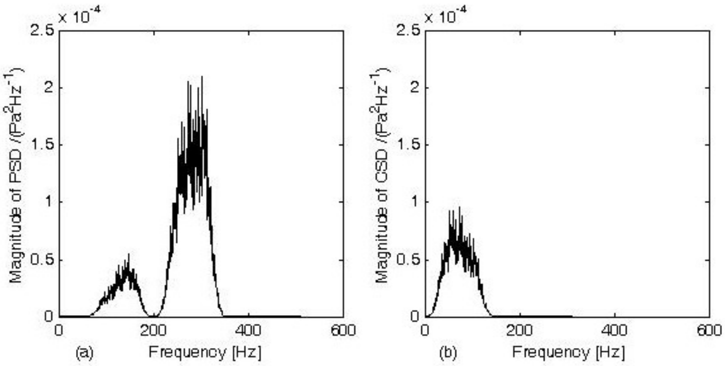

(a) PSD of the pressure signal. (b) CSD of pressure signal, α= 400 Hz

Figure 4. Analysis of the simulation acoustic pressure signal for reference point

3.2 The CYNAH reconstruction of sound field

A cylindrical hologram is set to “measure” the synthetically generating pressure in the sound field, which is 1.6m long with the radius 0.4m. The hologram is composed of 224 points with angle space $\Delta\theta=\pi/8$ radian and height space Δz=0.12m between the neighbouring points. The hologram is around the source surface axially. The reference point is assumed to be set at coordinates (0.35, 0, 0). The surface elements and nodes are set as shown in figure 2. The results of construction plotted in figure 5 are only for the nodes showed in figure 2, which locate on a generatrix of cylindrical surface, because the acoustic field is axially symmetrical. The reconstructed frequency is 50Hz under the cyclic frequency 400Hz. The reconstruction error is defined as $\varepsilon_m = \left\|S_{ss}^{\alpha} - S_a^{\alpha}\right\| / \left\|S_a^{\alpha}\right\| \cdot 100\%$, where S_{ss}^{α} and S_a^{α} are reconstructed CSD vector and analytical CSD vector, respectively, $\|\bullet\|$ is the norm operator. The reconstructed CSD function without any noise disturbance is shown in figure 5(a). The error is equal to 1.91% which is so accurate because of the lack of noise disturbance.

The reconstruction error increases when the noise is added to the synthetically generating pressure in the sound field. A zero means stationary random white-noise is added to the sound pressure on the hologram, which is independent of the sources and 10dB lower than the smallest sound pressure level on the hologram. The reconstructed CSD function on the surface is plotted in the figure 5(b). The error increases to 3.4% and the result is still satisfactory.

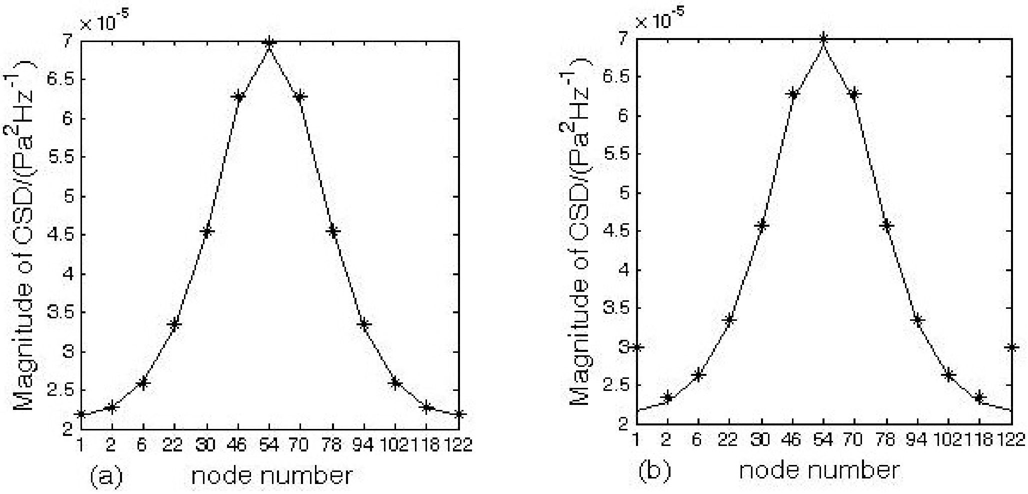

.(a) without disturbance of noise (b) disturbed by noise

’ ∗ ’ :computed, ‘——’: analytical

Figure 5. Reconstruction of CSD for cylindrical radiator at f=50Hz, with cyclic frequency α= 400 Hz

4. CONCLUSIONS

CYNAH based on BEM is developed for studying the information of acoustic field radiated from cyclo-stationary sources with irregular profiles. The BEM-based CYNAH algorithm extends the application of NAH method into cyclo-stationary sound field, especially for the acoustic sources with complicated profiles found frequently in internal combustion engines and rotating machinery. It is shown in simulation that the reconstructed sound filed agrees with the analytical one with quite well accuracy. The CSD hologram by CYNAH shows the location and feature of the modulating wave, which is helpful for understanding the modulating mechanism.

ACKNOWLEDGEMENTS

This work is aided by the Natural Science Fund of China (No. 10674096).

REFERENCES

[1] J. D. Maynard, E. G. Williams, Y. Lee, "Nearfield acoustic holograhy: I. Theory of generalized holography and the development of NAH", *Journal of the Acoustical Society of America* 78, 1395–1413 (1985).

[2] E. G. Williams, H. D. Dardy, "Generalized nearfield acoustic holography for cylinderal geometry: theory and experiment", *Journal of the Acoustical Society of America* 81, 389–407(1987).

[3] W. A. Veronesi, J. D. Maynard, "Digital Holographic Reconstruction of Sources with Arbitrarily Shaped surfaces", *Journal of the Acoustical Society of America* 85, 588-598(1989).

[4] M. Bai, "Application of BEM(boundary element method)-based acoustic holography to radiation analysis of sound sources with arbitrarily shaped geometries", *Journal of the Acoustical Society of America* 92, 533-549(1992).

[5] Z. Wang, S. F. Wu, "Helmholtz equation least squares method for reconstructing the acoustic pressure field", *Journal of the Acoustical Society of America* 102, 2020-2032 (1997).

[6] L. Song, G. Koopmann, J. Fahnline, "Numerical errors associated with the method of superposition for computing acoustic fields", *Journal of the Acoustical Society of America* 89, 2625-2633 (1991).

[7] J. Hald, "Time domain acoustical holography and its application", *Journal of Sound and Vibration* 35, 16-25(2001).

[8] W.A. Gardner, "Exploitation of spectral redundancy in cyclostationary signals", *IEEE Signal Processing Magazine* 8, 14–36(1991).

[9] G.K. Yeung, W.A. Gardner, "Search efficient methods of detection of cyclostationary signals", *IEEE Transactions on Signal Processing* 44, 1214–1223(1996).

[10] Q. Wan, W.K. Jiang, "Near field acoustic holography (NAH) theory for cyclostationary sound field and its application", *Journal of Sound and Vibration* 290, 956–967 (2006).

[11] Q. Wan, W.K. Jiang, "Near field acoustic holography for cyclostationary sound field and its partial source decomposition procedure", *Journal of Vibration and Acoustics, Transactions of the ASME* 127, 542-546(2005).

[12] E.G. Williams, et al., "Interior near-field acoustical holography in flight", *Journal of the Acoustical Society of America* 108, 1451–1463(2000).

[13] H. A. Schenck, "Improved integral formulation for acoustic radiation problems", *Journal of the Acoustical Society of America* 44, 42–58(1968).